Enhancement of the decay rate by plasmon coupling for Eu^{3+} in an Au nanoparticle model system

2011 EPL 93 57005

(http://iopscience.iop.org/0295-5075/93/5/57005)

epl A Letters Journal Exploring the Frontiers of Physics

March 2011

EPL, **93** (2011) 57005
doi: 10.1209/0295-5075/93/57005

www.epljournal.org

Enhancement of the decay rate by plasmon coupling for Eu^{3+} in an Au nanoparticle model system

J. T. van Wijngaarden, M. M. van Schooneveld, C. de Mello Donegá and A. Meijerink[a]

Debye Institute for Nanomaterials Science, Utrecht University - PO Box 80000, 3508 TA Utrecht, The Netherlands, EU

received 11 October 2010; accepted in final form 9 February 2011
published online 9 March 2011

PACS 78.47.jd – Time resolved luminescence
PACS 78.20.Ci – Optical constants (including refractive index, complex dielectric constant, absorption, reflection and transmission coefficients, emissivity)
PACS 78.55.Bq – Liquids

Abstract – 1Lanthanides are an interesting class of ions for applications in a variety of light-emitting materials because of their rich energy level structure. For many applications, control over the transition rates between specific energy levels is desirable, to be able to tune the emission output and the absorption strength. One method to achieve this is by bringing lanthanide ions close to a metal nanoparticle and use plasmon coupling to modify transition rates. In this letter we present measurements on a model system consisting of silica-coated gold nanoparticles for which lanthanide complexes have been incorporated in an amphiphilic layer surrounding the silica. We varied the thickness of the silica layer between 7.6 and 19.1 nm and incorporated the $Eu(TTA)_3$ complex in the surrounding amphiphilic layer. For the $^5D_0$ emission of Eu^{3+} we measured almost no decay rate enhancement with a 20 nm silica shell surrounding the Au particle, while for the thinnest shells we measured a decay rate enhancement up to a factor of five. Comparison with classical electromagnetic theory shows a good agreement between the experimentally observed enhancement and theory.

Introduction. – Lanthanides are an interesting group of elements because of their unique optical and magnetic properties, arising from the partially filled $4f$-shell. The lanthanides usually occur as trivalent ions which have a rich $4f^n$ energy level structure. Since the $4f$ electrons are shielded by the $5s$ and $5p$ electrons, there is only a weak influence from the environment on the position of the energy levels. This leads to sharp atomic-like transitions. Because of their interesting optical properties, lanthanides can be used for a wide range of applications, like light harvesting in solar cells [1,2], lighting [3], fluorescent lamps, white-light LEDs and displays, optical-signal processing [4] and bio-labeling [5]. For many of these applications, control over the luminescent properties is important. In spectral conversion processes for example, the transition rate between specific energy levels determines the efficiency for generating light of the desired wavelength. In the last decade it has been shown that noble-metal nanoparticles strongly interact with emitters and either enhance or quench their emission and absorption in different kind of geometries [6–9]. Metal nanoparticles (NPs) are well known for their optical properties, due to the collective oscillation of electrons, called plasmons [10,11]. If the oscillation is at resonance, the field radiated by the particle is much larger than the driving field, giving rise to a large field enhancement around the particle. An emitter placed close to a metal particle is influenced in two ways, if the transition energy is resonant with the plasmon oscillation [12].

Firstly, the enhanced field of the metal particle gives rise to a larger incoming field on the emitter, leading to an enhanced absorption. Secondly the field of the metal particle influences the decay rate of the emitter. This effect is sometimes called the Purcell effect, since already in 1946 he stated that the decay rates are dependent on the local environment [13]. This can be understood by looking at Fermi's golden rule, which states the the transition rate Γ can be expressed as

$$\Gamma = \frac{2\pi}{\hbar}|\langle g|\mathbf{p}|e\rangle|^2 \rho_p(\mathbf{r}_0, \omega), \quad (1)$$

[a]E-mail: a.meijerink@uu.nl

where $\langle g|\mathbf{p}|e\rangle$ is the transition dipole moment, and ρ_p the density of electromagnetic states. The latter depends on the electromagnetic field at the position of the emitter. Placing the emitter close to an object that interacts with the field of the emitter (*i.e.* changes the local density of states), leads to the modification of the decay rate [14]. This object can be a metal particle, but also an interface [15] or a cavity in which the emitter is placed [16].

In the past, interesting results have been published that demonstrate the modification of the emitted light as a function of metal-particle–emitter distance [6,7]. In both papers the authors were able to measure single-molecule emission intensity close to a scanning metal tip. Due to this well-defined geometry, a good agreement between experiment and theory was obtained, with a luminescence enhancement for decreasing tip-emitter distance up to a few nanometers. For even smaller distances quenching of the luminescence is expected, which was also observed [17–19].

In addition to coupling between plasmons in macroscopic metallic structures (metal tips of films) also plasmon enhancement of the radiative and non-radiative decay induced by metal nanoparticles has been reported for fluorescent molecules and quantum dots [9,20–24].

If we want to measure similar effects for lanthanide ions, we need to take a different approach. Since Ln^{3+} ions have lower-absorption cross-sections and slower decay rates, the intensity is too low for single-emitter experiments. It is still possible to place an ensemble of emitters close to a metal particle, but it is a challenge to have all emitters at the same and well-defined distance. Already since the 1970s experiments were done, demonstrating plasmon enhanced decay rates for transitions on lanthanide ions close to metal surfaces [15,25,26]. In more recent research enhanced Er^{3+} luminescence was measured, due to the presence of anisotropic Ag particles [27], or by placing the Er ions in a coaxial metal resonator [28]. In these geometries there is limited control over the distance between the emitter and the silver nanostructure. By varying the implantation depths, the distance can be varied but there is large variation in distances due to the width of the implantation profile. Control over the coupling between the emitter and the metal structure is provided by tuning the overlap between the plasmon resonance and the emission wavelength. More recently, studies have appeared where the distance dependence of plasmon resonance enhancement was studied for lanthanide complexes and silver nanoparticles of silver island films [29,30]. In this paper we will present a model system to investigate the plasmon coupling for Ln^{3+} emission, in which the distance between the Ln^{3+} ion and the metal particle can be tuned. We will use spherical gold nanoparticles (NP), coated with a silica layer ($Au@SiO_2$). The thickness of the silica can be tuned and thereby we control the distance between the emitters at the surface and the metal NP. The lanthanide ions are placed at the surface by coating the $Au@SiO_2$ particles with an amphiphilic layer, in which hydrophobic europium complexes are inserted. The emission lines of europium have a fairly good overlap with the plasmon resonance of Au NPs. Moreover the ligand of the complex acts as a sensitizer for the Eu^{3+} emission. Excitation takes place in the UV, where there is no overlap with the plasmon resonance, followed by efficient energy transfer (ET) to the $^5D_0$ level of the Eu^{3+} ion. This gives the opportunity to only look at modification of the decay rate of the Eu^{3+} $^5D_0$ emission in the red part of the spectral region. We will show a decay rate enhancement up to five times for a silica shell thickness of 7.6 nm. Our experimental results are well reproduced by classical electromagnetic theory.

Experimental. –

Sample preparation. Spherical gold particles were synthesized via a citrate reduction method [31], that was modified to grow larger particles via a seeded growth method [32]. The seeds were made by injecting a solution of sodium citrate to a boiling solution of Au salt ($HAuCl_4$), under vigorous stirring. The average diameter of the seeds varied between 12 and 14 nm for different batches. Further growth of the seeds was done by simultaneous injection of seeds and citrate solution into a boiling Au salt solution under vigorous stirring. The solution was boiled for one hour, after which more citrate was added for stabilization. By varying the amount of seeds, the Au particle size can be controlled. The particles are stable in water for at least a month.

The Au particles were coated with silica as described in detail in ref. [33]. In short: poly-(vinylpyrrolidone) (PVP) was absorbed on the Au particles. After several washing steps to remove the excess PVP the particles were transferred to a solution of ammonia in ethanol. Silica shells of different thicknesses were grown by adding various amounts of tetraethoxysilane (TEOS).

Europium complexes were attached on the $Au@SiO_2$ particles, after applying an amphiphilic coating, synthesized according to ref. [34]. Figure 1 schematically shows the preparation steps. $Au@SiO_2$ particles were made hydrophobic by coating them with octadecanol (ODOH) via a condensation reaction. The particles were transferred to chloroform and the europium complex ($Eu(TTA)_3$ [35]) and PEG molecules (see fig. 2) were added in 35 times excess with respect to a full surface area covering of the $Au@SiO_2$ particles. The mixture was added drop-wise to water which was heated to $\sim$80 °C and vigorously stirred. At this temperature the chloroform evaporates and the PEG forms micelles around the $Au@SiO_2$ particles, with Eu complexes incorporated in the hydrophobic tails. We will further call these particles $Au@SiO_2@Eu(TTA)_3$. Due to the excess of PEG and Eu complex added, also empty micelles were formed. These empty micelles were removed by centrifugation, and used for reference measurements.

Measurements. Au nanoparticles were characterized using transmission electron microscopy (TEM, Philips Tecnai 10). Optical absorption spectra were recorded with

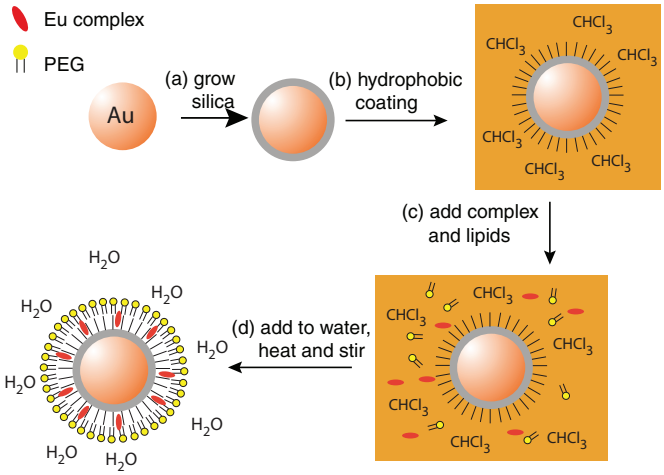

Fig. 1: Schematic representation of sample preparation. Gold particles are subsequently coated with silica (a) and octadecanol (ODOH) (b). The amphiphilic PEG molecules and Eu complex are added (c) and this mixture is drop-wise added to water (d). Due to heating and mixing, the chloroform evaporates, leaving a water-soluble PEG-coated $Au@SiO_2$ particle with the Eu complex incorporated in the amphiphilic layer.

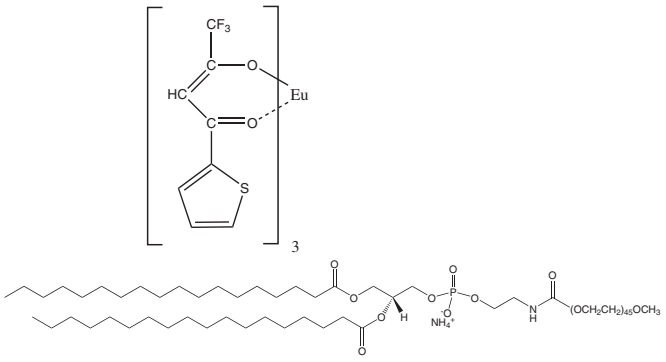

Fig. 2: Molecular structure of the europium complex (Eu(thenoyltrifluoroacetonate)$_3$ $2H_2O$ ($Eu(TTA)_3$), top) and the amphiphilic PEG molecules (18 : 0 PEG2000 PE, bottom).

a Perkin-Elmer Lambda 950 UV/Vis/IR absorption spectrometer. Emission and excitation spectra were measured using an Edinburgh Instruments FLS920 fluorescence spectrometer with a Hamamatsu R928 photomultiplier tube (PMT). As excitation source a 450 W Xe lamp was used. Luminescence decay measurements were performed under pulsed excitation with a LPD3000 dye laser (p-terphenyl dye, 350 nm), pumped by a Lambda Physik LPX100 excimer laser (XeCl, 308 nm). Decay curves were recorded using either the multi-channel scaling technique, incorporated in the FLS920 system, or with a digital oscilloscope (Tektronix 2440).

Results. –

Sample characterization. Figure 3(a)–(d) shows TEM images of $Au@SiO_2$ particles. The average Au core

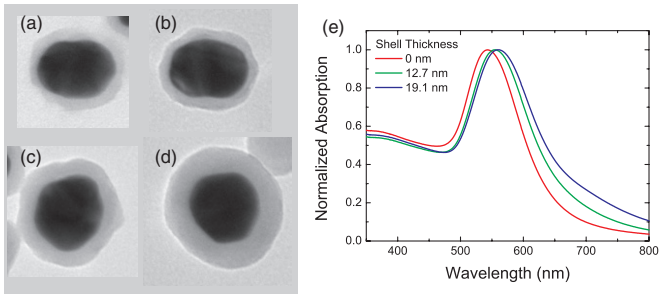

Fig. 3: TEM images of $Au@SiO_2$ particles, with shell thicknesses of 7.6 nm (a), 9.5 nm (b), 12.7 nm (c) and 19.1 nm (d). The average core diameter is 60 nm. (e) shows the absorption spectra of Au particles (red line) and $Au@SiO_2$ particles (green line = 12.7 nm, blue line = 19.1 nm).

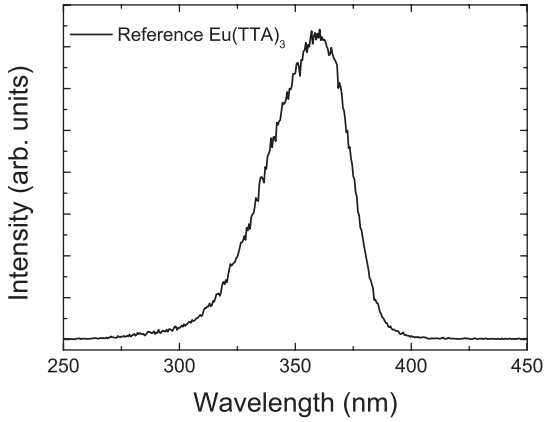

Fig. 4: Excitation spectrum of $Eu(TTA)_3$ in micelles without $Au@SiO_2$, for the $^5D_0 \rightarrow {}^7F_2$ emission at 610 nm, $T = 300$ K.

diameter is 60 nm and the silica shell thicknesses are 7.6, 9,5, 12.7 and 19.1 nm for (a) to (d), respectively. Figure 3(e) shows the absorption spectra for Au (red line) and $Au@SiO_2$ (green line = 12.7 nm, blue line = 19.1 nm), with the plasmon resonance around 550 nm, characteristic for spherical gold particles. The resonance shifts to longer wavelengths for increasing shell thickness. This is attributed to the change in refractive index, due to the shell surrounding the particles (1.32 for water and 1.45 for silica) and has been observed before [36].

Emission and decay measurements. Figure 4 shows an excitation spectrum of a reference sample of empty PEG micelles with the Eu complex for the $^5D_0 \rightarrow {}^7F_2$ emission at 610 nm. The broad excitation band is assigned to excitation into the singlet states of the ligand. From these states the energy is transferred to the Eu^{3+} ion. Samples with Au NP in the micelles show a similar spectrum. Comparison with fig. 3 shows that the excitation band is off-resonance with the plasmon resonance of the Au particles. However at this wavelength there is significant absorption due to interband transitions in the Au. The strong competing absorption by the gold NP around 350 nm reduces the emission intensity from the Eu complex.

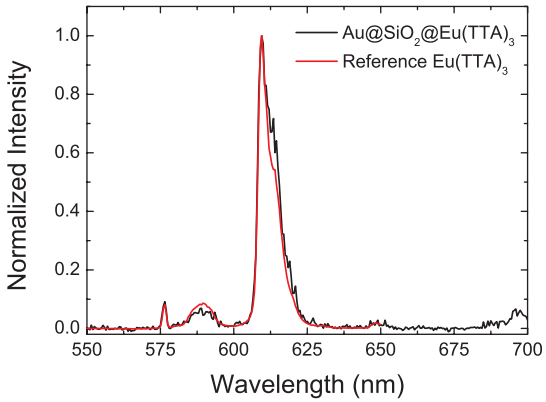

Fig. 5: Normalized emission spectra for $Au@SiO_2@Eu(TTA)_3$ (black line, silica shell thickness of 12.7 nm) and a $Eu(TTA)_3$ reference (red line) upon excitation at 350 nm.

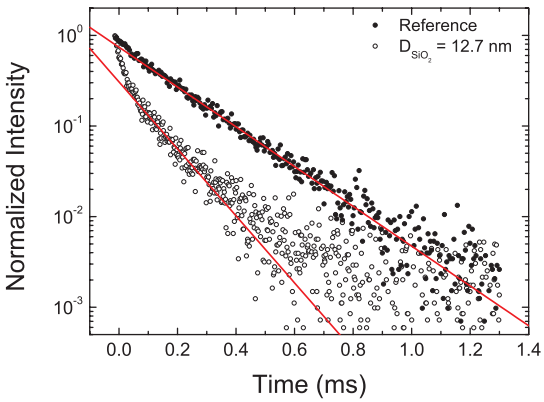

Fig. 6: Decay traces for the Eu^{3+} emission in a reference sample (empty micelles) and an $Au@SiO_2@Eu(TTA)_3$ sample, with a SiO_2 shell thickness of 12.7 nm. Red lines are fits to the data. The initial fast decay of the $Au@SiO_2@Eu(TTA)_3$ sample is not attributed to Eu^{3+} luminescence.

Figure 5 shows emission spectra for $Au@SiO_2@Eu(TTA)_3$ (black line) and the reference sample without $Au@SiO_2$ (red line), upon excitation at 350 nm. The silica shell thickness is 12.7 nm. The spectra are normalized at the ${}^5D_0 \rightarrow {}^7F_2$ emission. No clear differences between these spectra are observed. The low signal-to-noise ratio, due to the low Eu^{3+} signal in the $Au@SiO_2@Eu(TTA)_3$ sample can be attributed to either competitive absorption (see above) or to the low complex concentration. To prevent the sample to become opaque at either the excitation or the emission wavelength, we measured on diluted samples (conc. $\simeq 0.05$ nM). It is not possible to make an absolute comparison between sample emission intensities because of the large uncertainty in the amount of complex incorporated in the samples.

No effect on the branching ratio (*i.e.* the relative intensities) of the emission lines is observed in fig. 5. This is probably due to the fact that there is overlap between all the emission lines and the plasmon resonance, which has a tail that extends to 700 nm. The effect on the relative emission intensities will therefore be small, and the observation of the effect is difficult since the emission spectra have a low signal-to-noise ratio. It would therefore also be interesting to use lanthanides with a larger spectral spread of emission lines, for example Tb^{3+}.

To investigate the modification of the transition probabilities by plasmon coupling, luminescence decay traces were recorded. Figure 6 shows decay traces of the Eu^{3+} ${}^5D_0 \rightarrow {}^7F_2$ emission, for a sample with a silica shell thickness of 12.7 nm and the corresponding reference sample with empty micelles containing $Eu(TTA)_3$. The emission from the reference sample shows a single exponential decay of 197 μs. The sample containing the $Au@SiO_2@Eu(TTA)_3$ NPs shows a bi-exponential decay. The fast-decay component is only observed in some samples where the Eu^{3+} emission intensity is very low. It is attributed to scattered laser light reaching the detector, or weak and fast emission from unidentified species in the sample. The slow component is assigned to emission from Eu^{3+} complexes in the $Au@SiO_2@Eu(TTA)_3$ NPs. The red lines are single exponential fits to the decay of the Eu^{3+} emission. The decay times were determined by fitting the time dependence of the intensity to a single exponential decay. The time interval was chosen starting at 0.1 ms to prevent an influence of the initial fast decay. The deviation at longer time scales is due to the background, which was not included in the fitting procedure. The decay time obtained from the fit is $\tau_{Au} = 117\,\mu$s, which is significantly faster than for the reference sample. We attribute the enhancement of the Eu^{3+} decay to the presence of the Au particle.

We determined the enhancement of the total decay rate by dividing the decay time of the Eu^{3+} emission for the reference sample by the decay time for the $Au@SiO_2@Eu(TTA)_3$ sample. For the results displayed in fig. 6, this gives an enhancement of: $\tau_{ref}/\tau_{Au} = 197/117 = 1.7$. Concentration effects can also have an influence on the decay time, for example due to concentration quenching. To exclude this effect, we aimed to keep a low concentration of the Eu complex. The estimated minimum distance between the complexes is $\sim$1 nm. Moreover we used the empty micelles created in the synthesis of the measured sample as reference. These have a similar complex concentration, thus possible concentration effects are corrected for.

For a range of silica shell thicknesses we measured the Eu^{3+} emission decay curves and calculated the enhancement factors. Figure 7 shows the enhancement *vs.* the silica shell thickness. For larger emitter NP distance (larger silica shell thickness) the decay rate enhancement is nearly one, meaning that there is almost no effect, as expected. For decreasing emitter particle distance the enhancement effect becomes larger, up to an enhancement of almost five at a shell thickness of 7.6 nm. We calculated the expected enhancement which is shown by the grey line in fig. 7. Classical electromagnetic Mie theory was used for this [37,38],

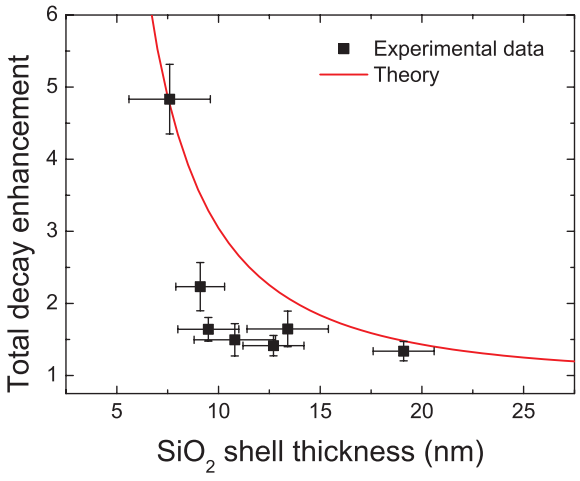

Fig. 7: Enhancement factor of the total decay rate of the Eu^{3+} emission as a function of the SiO_2 shell thickness. The red line is the calculated enhancement, using Mie theory [37,38].

with input parameters the diameter of the particle $d = 60\,\text{nm}$, the emission wavelength $\lambda = 610\,\text{nm}$, the initial quantum efficiency without the presence of Au of 10% and the bulk optical constants of gold [39]. The theoretically calculated enhancement factor is somewhat underestimated for the thicker silica shells due to the redshift of the plasmon resonance for increasing silica shell thickness (see fig. 3(e)) which causes a better overlap with the strongest Eu^{3+} emission line at 610 nm. The enhancement factor contains contributions from both radiative and non-radiative decay. Especially for the smallest shell thickness (7.6 nm) non-radiative decay contributes strongly to the total decay enhancement factor of 5.

There is a fairly good agreement between the experimental results and the theory, although we measured a smaller enhancement than expected. A possible explanation is that the actual distance between the Eu^{3+} ion and the Au NP is slightly larger than the SiO_2 layer. The Eu complex is incorporated in the hydrophobic part of the PEG layer. The ODOH and the PEG molecules have a length of approximately 1 nm and 2 nm, respectively, which adds $\sim$2 nm to the distance. Also note that the calculations are done for spherical particles, while fig. 3 shows that the particles are not perfectly spherical.

Conclusions. – In this letter the enhancement of the total decay rate of the Eu^{3+} emission due to plasmon coupling has been investigated. A model system has been used where the distance between an Eu complex and Au nanoparticles is the same for all Eu complexes. To achieve this, Eu complexes are incorporated in an amphiphilic layer around an Au-core silica-shell nanoparticle. By varying the thickness of the silica layer, the distance between the Eu complex and the Au NP has been varied between 7.6 and 19.1 nm. For the smallest distance a fivefold increase in decay rate is observed. Increasing the distance results in a decrease of the enhancement, in fairly good quantitative agreement with theory.

* * *

This work is part of the Joint Solar Programme (JSP) of the Stichting voor Fundamenteel onderzoek der Materie (FOM), which is part of the Nederlandse Organisatie voor Wetenschappelijk onderzoek (NWO). The JSP is co-financed by gebied Chemische Wetenschappen of NWO and stichting Shell Research.

REFERENCES

[1] Richards B. S., *Sol. Energy Mater. Sol. Cells*, **90** (2006) 1189.
[2] van der Ende B., Aarts L. and Meijerink A., *Phys. Chem. Chem. Phys.*, **11** (2009) 11081.
[3] Jüstel T., Nikol H. and Ronda C., *Angew. Chem., Int. Ed.*, **37** (1998) 3084.
[4] Polman A., *J. Appl. Phys.*, **82** (1997) 1.
[5] Sabbatini N., Guardigli M. and Lehn J., *Coord. Chem. Rev.*, **123** (1993) 201.
[6] Anger P., Bharadwaj P. and Novotny L., *Phys. Rev. Lett.*, **96** (2006) 113002.
[7] Kühn S., Håkanson U., Rogobete L. and Sandoghdar V., *Phys. Rev. Lett.*, **97** (2006) 017402.
[8] Tam F., Goodrich G., Johnson B. and Halas N., *Nano Lett.*, **7** (2007) 496.
[9] Dulkeith E., Ringler M., Klar T. and Feldmann J., *Nano Lett.*, **5** (2005) 585.
[10] Kreibig U. and Vollmer M., *Optical Properties of Metal Clusters* (Springer, Berlin) 1995.
[11] Bohren C. F. and Huffman D. R., *Absorption ad Scattering of Light by Small Particles* (Wiley-VCH) 2004.
[12] Bharadwaj P., Deutsch B. and Novotny L., *Adv. Opt. Photon.*, **1** (2009) 438.
[13] Purcell E. M., *Phys. Rev.*, **69** (1946) 681.
[14] Sprik R., van Tiggelen B. A. and Lagendijk A., *Europhys. Lett.*, **35** (1996) 265.
[15] Drexhage K., *J. Lumin.*, **1-2** (1970) 693.
[16] Kleppner D., *Phys. Rev. Lett.*, **47** (1981) 233.
[17] Lakovicz J. R., *Anal. Biochem.*, **337** (2005) 171.
[18] Lakovicz J. R., *Plasmonics*, **1** (2006) 5.
[19] Lee S. Y., Nakaya K., Hayashi T. and Hara M., *Phys. Chem. Chem. Phys.*, **11** (2009) 4403.
[20] Kulakovich O., Strekal N. and Yaroshevich A., *Nano Lett.*, **2** (2002) 1449.
[21] Pons T., Menditz I. L. and Sapsford K. E., *Nano Lett.*, **7** (2007) 3137.
[22] Dulkeith E., Morteani A. C., Niedereichholtz T., Klar T. A. and Feldmann J., *Phys. Rev. Lett.*, **89** (2002) 03002.
[23] Gueroui Z. and Libcaber A., *Phys. Rev. Lett.*, **93** (2004) 166108.
[24] Fedutik Y., Temnov V. V., Schöps O., Woggon U. and Artemyev M. V., *Phys. Rev. Lett.*, **99** (2007) 136802.
[25] Amos R. M. and Barnes W. L., *Phys. Rev. B*, **55** (1997) 7249.

[26] Kalkman J., Kuipers L., Polman A. and Gersen H., *Appl. Phys. Lett.*, **86** (2005) 041113.
[27] Mertens H. and Polman A., *Appl. Phys. Lett.*, **89** (2006) 211107.
[28] Kroekenstoel E. J. A., Verhagen E., Walters R. J., Kuipers L. and Polman A., *Appl. Phys. Lett.*, **95** (2009) 263106.
[29] Wang Y., Zhou X., Wang T. and Zhou J., *Mater. Lett.*, **62** (2008) 3582.
[30] Zhang J., Fu Y. and Lakovicz J. R., *J. Phys. Chem. C*, **113** (2009) 19404.
[31] Frens G., *Nature Phys. Sci.*, **241** (1973) 20.
[32] Liu S. H. and Han M. Y., *Adv. Funct. Mater.*, **15** (2005) 961.
[33] Graf C., Vossen D. L. J., Imhof A. and van Blaaderen A., *Langmuir*, **19** (2003) 6693.
[34] Koole R., van Schooneveld M. M., Hilhorst J., Castermans K., Cormode D. P., Strijkers G. J., de Mello Donegá C., Vanmaekelbergh D., Griffioen A. W., Nicolay K., Fayad Z. A., Meijerink A. and Mulder W. J. M., *Bioconjug. Chem.*, **19** (2008) 2471.
[35] Malta O. L., Brito H. F., Menezes J. F. S., Gonçalves e Silva F., Alvers S. jr., Farias F. S. jr. and de Andrade A. V. M., *J. Lumin.*, **75** (1997) 255.
[36] Bardhan R., Grady N. K. and Halas N. J., *Small*, **4** (2008) 1716.
[37] Mertens H., Koenderink A. F. and Polman A., *Phys. Rev. B.*, **76** (2007) 115123.
[38] Kim Y. S., Leung P. T. and George T. F., *Surf. Sci.*, **195** (1988) 1.
[39] Johnson P. B. and Christy R. W., *Phys. Rev. B.*, **6** (1972) 4370.